Energy Science, Engineering and Technology

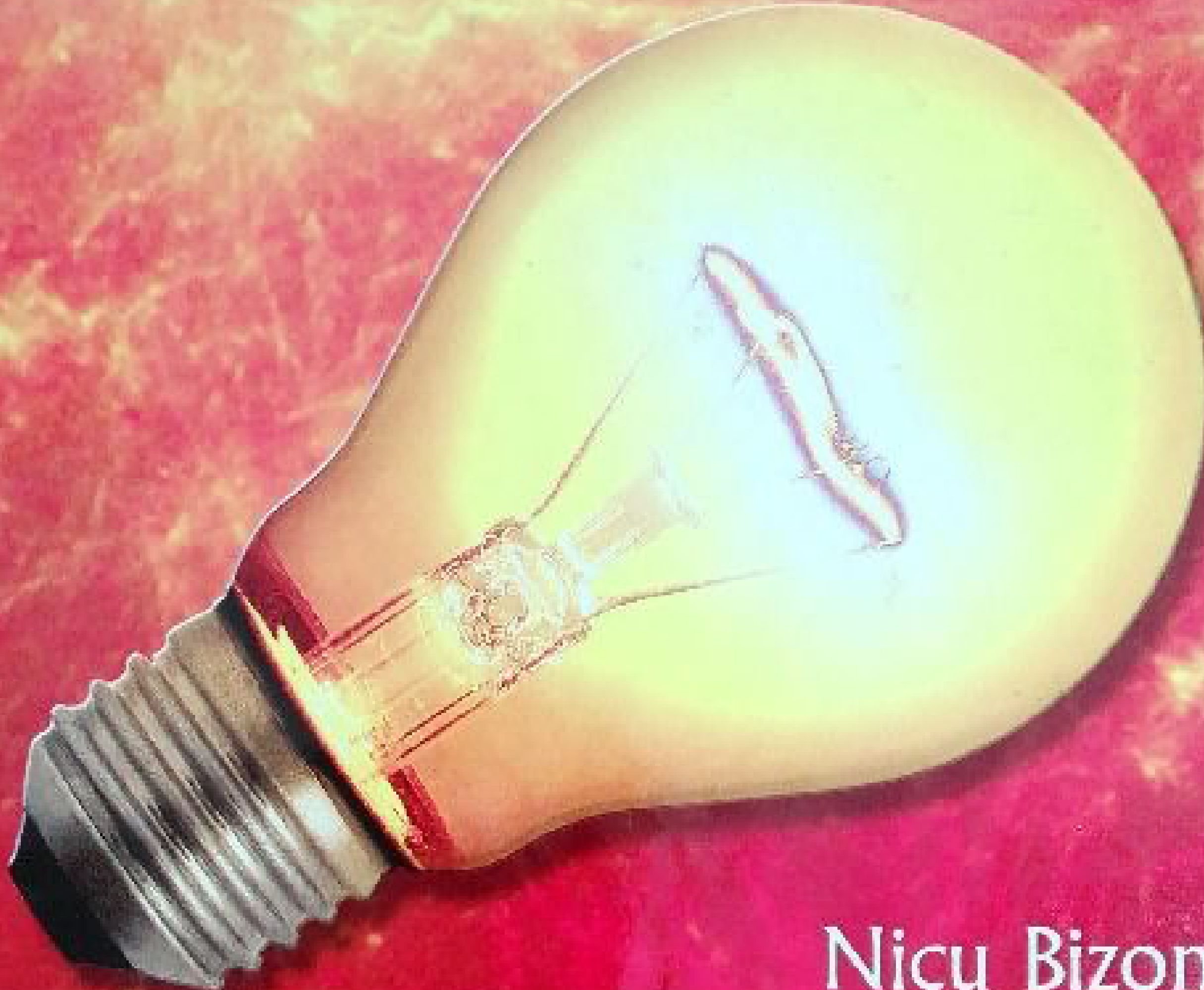

Nicu Bizon
Naser Mahdavi Tabatabaei
Editors

Advances in Energy Research

Energy and Power Engineering

NOVA

PWM CYCLOCONVERTER – AN ENERGY EFFICIENT TOPOLOGY FOR FUEL CELL INVERTER SYSTEMS

Nicu BIZON Marian RADUCU Mihai OPROESCU
Department of Electronics, Computers and Electrical Engineering,
Faculty of Electronics, Communications and Computers, University of Pitesti, Romania,
nicu.bizon@upit.ro, marian.raducu@upit.ro mihai.oproescu@upit.ro

Abstract
Firstly, in this chapter will be presented some advanced topologies of Fuel Cell (FC) inverter systems, which are proposed for an efficient operation of FC stack and to assure a high reliability of system, too. The case of FC inverter systems used in Distributed Generation (DG) applications and vehicle applications is considered. The operation conditions and the performance indicators for efficient operation and high reliability are defined for both cases.
Secondly, in this chapter is analyzed a PWM cycloconverter topology with multiple-carrier control technique. The simulation results successfully showed the good performances obtained for Total Harmonics Distortion (THD) coefficient. Finally, some experimental results are shown for a PWM cycloconverter and last section concludes the chapter.

Keywords
Hybrid Power Source, Fuel Cell, Energy Storage Device, Inverter, PWM Cycloconverter, THD.

1. Introduction
As it is known, the Polymer Electrolyte Membrane Fuel Cell (PEMFC) stack represents one of the most used solutions as DC energy source in Energy Generation System (EGS). Consequently, depending of load type, which can be AC or DC, the fuel cell EGS must be a power converter of type DC-AC or DC-DC, respectively. The power conversion may be done in one stage or in multi-stages. For reason of EGS efficiency, the number of energy conversion stages should be minimized. Consequently, the PWM cycloconverter topology could represent an energy efficient solution for this point of view. Also, for reason of PEMFC reliability and reduction of the fuel consumption, the power conversion stage may be multi-port type that use as auxiliary energy source on the second input port a hybrid Energy Storage Device (ESD) (a hybrid stack of batteries and/or ultracapacitors).
The PEMFC EGS can be used in residential application (grid connected or not) or in vehicle applications because of its features: small size and ease of construction, a fast start-up and low operating temperature. Unfortunately, its relatively short life represents a major disadvantage that reduces their commercialization [1]. The load for the fuel cell EGS grid connected is of AC type, so the inverter system must be the last power conversion stage (Figure 1).
As it is known, the ripple of the inverter current is the main factor for low performance in operating of PEMFC stack. The operating performances are defined at level of energy efficiency [2, 3, 4] and PEMFC life cycle [2, 5, 6]. Also, for the PEMFC current ripple it is known that the spectral components of low frequency (LF) (LF harmonics) affect in much measure the PEMFC life cycle than spectral components of high frequency (HF) (HF harmonics) and contribute with up to 10% reduction in the available output power [7, 8].

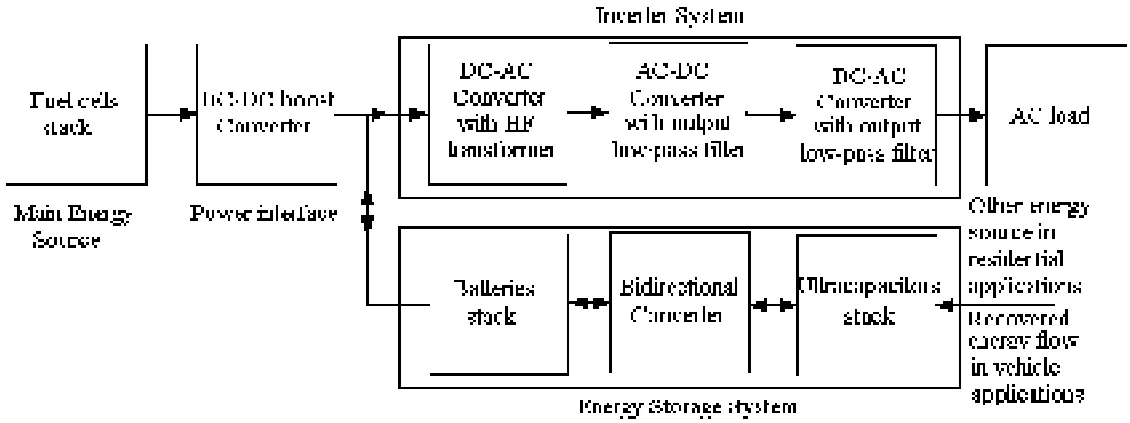

Figure 1. Basic EGS topology with the inverter system powered by a fuel cell stack: adapted from [2]

Consequently, it is necessary to be specified for each frequency band some restrictions for the spectral component's magnitude of the PEMFC current ripple. These limits were given in frequency domain [9] or in time domain. In time domain, the Ripple Factor (RF) represents a performance indicator that is usually used to define such of limits:

$$RF_I = \frac{I_{max} - I_{min}}{I_{(AV)}} \tag{1}$$

where I_{max}, I_{min}, and $I_{(AV)}$ are the value of maximum, minimum and average, respectively.

New reliability limits that are specified by the RF must be lower than 5% [10]. The interleaved technique can be a solution to mitigate the ripple of PEMFC current and subsequently to reduce the RF under mentioned limit [11, 12].

In PEMFC EGS applications, the variations of the load power below grid frequency (50 or 60 Hz) represent "load following" action of the EGS control. Consequently, the power flow supplied by PEMFC stack must change after the load variation. For dynamical load, with variations in time shorter than the time constant of PEMFC, the control of the PEMFC stack can't force the stack to delivery power necessary to that kind of load, if only this is used as energy source. So, a ESD stack, which is dimensioned only for these load transitions, is necessary to be used in order to avoid the phenomenon of fuel starvation [13, 14, 15]. The PEMFC control should track to within 1% the Maximum Power Point (MPP) of PEMFC stack for purposes of both reliability and efficiency [16, 17, 18]. Consequently, the topology of Hybrid Power Source (HPS) with a MPP tracking controller can be o solution (Figure 2) [19].

As it was mentioned above, the use of the ESD is needed in PEMFC HPS topologies to assure the power balance under dynamic load, taking in account the different response time of the ESD used (usually, a hybrid stack of batteries and ultracapacitors). The power of PEMFC stack (P_{FC}) and ESD stack (P_{ESD}) assure the power flow on the low voltage (LV) DC bus (P_{load}) via the MPP boost converter (P_1) and the bidirectional converter (P_2), respectively. The power balance at the HPS output is given by relationship $P_{load} \cong P_1 + P_2$, where the load power flow, P_{load}, is the input power for the inverter system, which can be modeled as an equivalent load. The power flows management is performed by the MPP controller and LV DC bus controller, respectively. The fuel cell MPP current (I_{MPP}) is tracked in an adaptive feedback loop by injecting a probing current [19] or by using other control techniques. As it is known, the power ripple becomes lowest when the operation point gets closer to MPP.

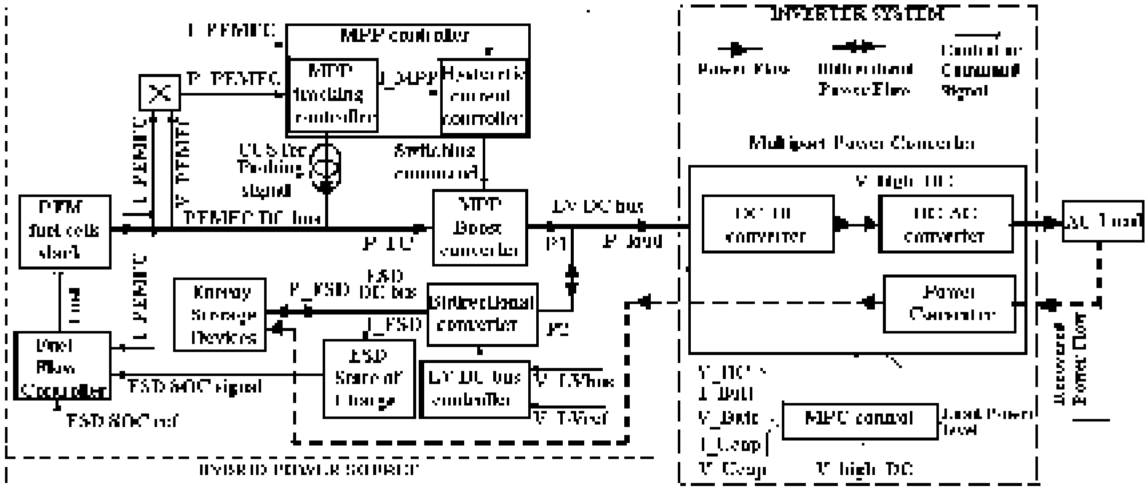

Figure 2. Fuel cell HPS topology with MPP tracking controller: adapted from [2]

In FC vehicle applications, high energy demands can appear for a short time. These power peaks will cause high slopes of PEMFC current and, subsequently, the voltage drops appear. The ESD are required to compensate these power peaks of load and also to absorb the energy from the regenerative braking or other recovered power flows. The current slopes are given experimentally for different PEMFC stacks, depending on their power (about 10 A/s per each kW power) [20, 21]. For improving the reliability of PEMFC stack, it is obviously that ESD and PEMFC technologies need to be merged in HPS. Usually, a HPS combines one or more energy sources with mixed ESD that operate together to deliver power (to the DC load or into the AC grid via the inverter system) or to store energy. This permits reduction of the hydrogen consumption and a reliable fuel cell HPS operating under sharp power pulses [22, 23, 24]. The challenge for control of power flows in fuel cell HPS is to enhance all performance indicators through its technologies that working together. Some fuel cell HPS structures of type FC/ultracapacitor [25, 26], FC/battery [27] and FC/ultracapacitor/battery [28] have already reported.
Some typical topologies of fuel cell inverter systems are presented below, in Figures 3 and 4. If the power of AC load is relative constant, then a fuel cell EGS topology without ESD may be used (Figure 3). The inverter system is powered directly by the fuel cells stack and the ESD capacity is reduced or even canceled. The inverter efficiency increases if the stages number of energy conversion should be minimized (Figure 4).

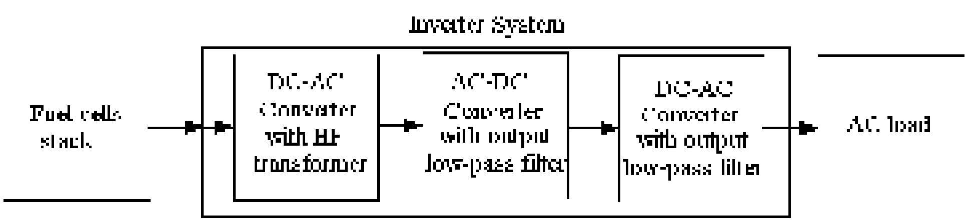

Figure 3. Three-stages inverter system powered directly from the PEMFC stack

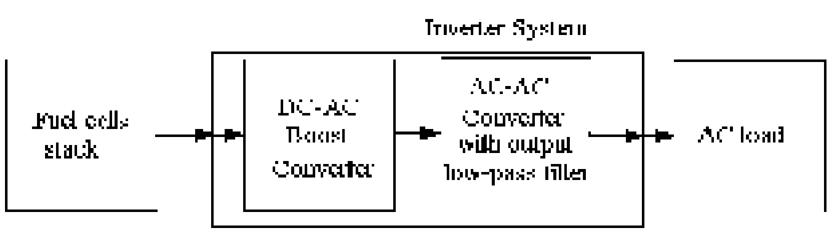

Figure 4. Two-stages inverter system powered directly from the PEMFC stack

Considering Figure 2, if State of Charge (SOC) of ESD is in its admissible range, then the fuel flow level is controlled by the fuel cell current. Consequently, the fuel flow controller assures the fuel rate that is necessary to supply the dynamic load and the MPP is variable in time. When the stationary load regime is reached, the fuel flow controller assures a constant fuel rate. For a given load sequence a fuel rate sequence is obtained.

2. PWM Cycloconverter Topology

This section presents an investigation of the PWM cycloconverter operation that can be used into an Energy Generation System (EGS) as power interface between the HF AC bus and the AC output load (see Figure 4). To minimize the price of inverter system, measured in $/W, is necessary to reduce the power processing stages [29, 30]. One of the solutions is to remove the high DC bus. Consequently, following the DC-DC power interface, the inverter design includes a forward converter (he DC-AC converter) coupled with a cycloconverter (the AC-AC converter), as is shown in Figure 5. In fact, the forward converter represents a square DC-AC source that produces a HF AC voltage bus from the LV DC voltage bus. The rectifier bridge and the capacitive filter that were used on HV DC voltage bus have been removed.

The PWM cycloconverter generates AC power for the AC load or for the local AC grid (Figure 5). The AC output voltage amplitude can be stabilized using a well designed PI control (not presented in Figure 5). The feedback control loop presented in Figure 5 must assure an easy grid connection of the EGS.

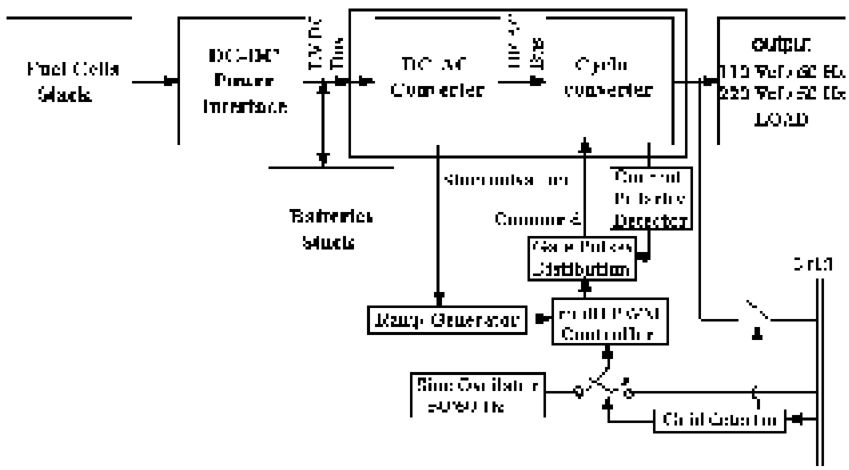

Figure 5. Use of the PWM cycloconverter for generation of an AC local grid

Working frequency of the DC-AC converter, which is also the frequency of the HF AC bus, is reduced according to the thyristors performances. For example, a frequency in range of 1 to 5 kHz gives as a reduced output spectrum, so the output voltage quality can be assured. If a 1 kHz carrier frequency is used to generate the 220Vef/50Hz output grid voltage, then exactly 20 command pulses per a grid period are necessary. It will be shown that this yet assures an acceptable power spectral quality, measured by the Total Harmonics Distortion (THD) coefficient. But also it will be shown that the cycloconverter behavior is strongly dependent by the load quality factor, especially for light load.

The cycloconverter topology consists of eight unidirectional switches (thyristors) coupled in four bidirectional switches in a full bridge (Figure 6).

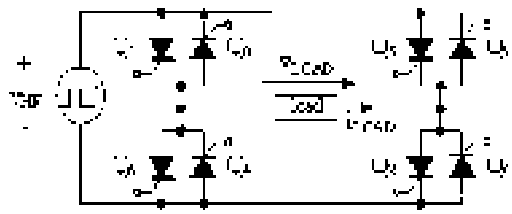

Figure 6. Cycloconverter topology

The multi-carried PWM technique allows the cycloconverter topology to be a low-cost solution for medium power EGS (with power in range of 1 to 10 kW). It was showed that the cycloconverter using a multi-carrier PWM controller can produce AC power as conventional inverter with pure sine PWM controller [31, 32]. A two-carrier PWM controller was implemented for simulations and experiment (Figure 7).

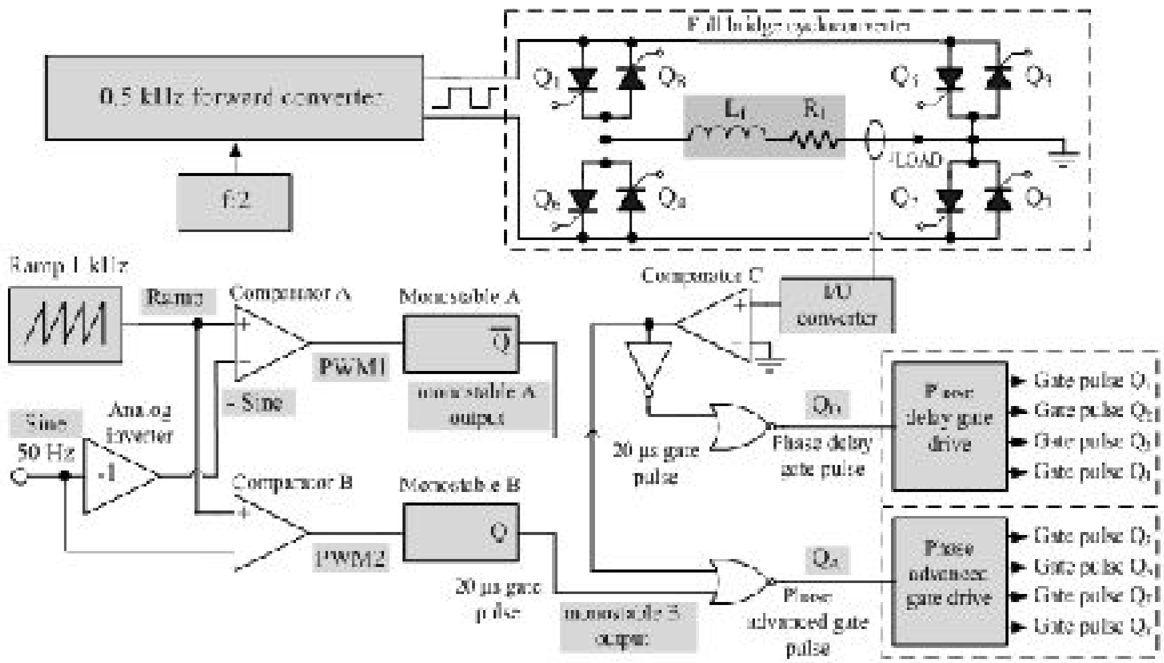

Figure 7. Two-carrier PWM controller

3. PWM Cycloconverter Operation

In Figure 7 was shown the PWM cycloconverter implemented in this section. The multiple-carrier PWM methods lead to HF inverters that are simple to control as are the conventional PWM inverters. These inverters can support natural commutation, thus the wave-forms can be determined directly from the well known PWM process. To generate a conventional PWM sequence, a ramp carrier is compared with a modulating function of sine type, as shown in Figure 8. The names of the waveforms are the same as those shown in Figure 7.

From top to bottom are presented the waveforms that shown the operation of the PWM cycloconverter. The first plot shown the ramp and the sine waveform that are compared and the result of comparison is the PWM2 signal. This signal is applied to the *B* monostable, which provides to its output a pulses sequence. The Q_A command (gate pulses with phase delay) is identically with the output of the *B* monostable if the load current is negative, else Q_A is zero. In the next plots the PWM1 signal is obtained by comparison of the ramp and the opposite sine waveform (- sine). This signal is applied to the *A* monostable, which provides to its output a pulses sequence. The Q_D command (gate pulses with phase advanced) is

identically with the output of the *A* monostable if the load current is positive, else Q_D is zero. Q_A and Q_D are gate sequences for the full-bridge of thiristors.
The frequency for the HF AC bus is a half of the ramp frequency. These two signals must be in phase, and synchronized with grid frequency if it is the case.
In the last plot is shown the output voltage and load current.

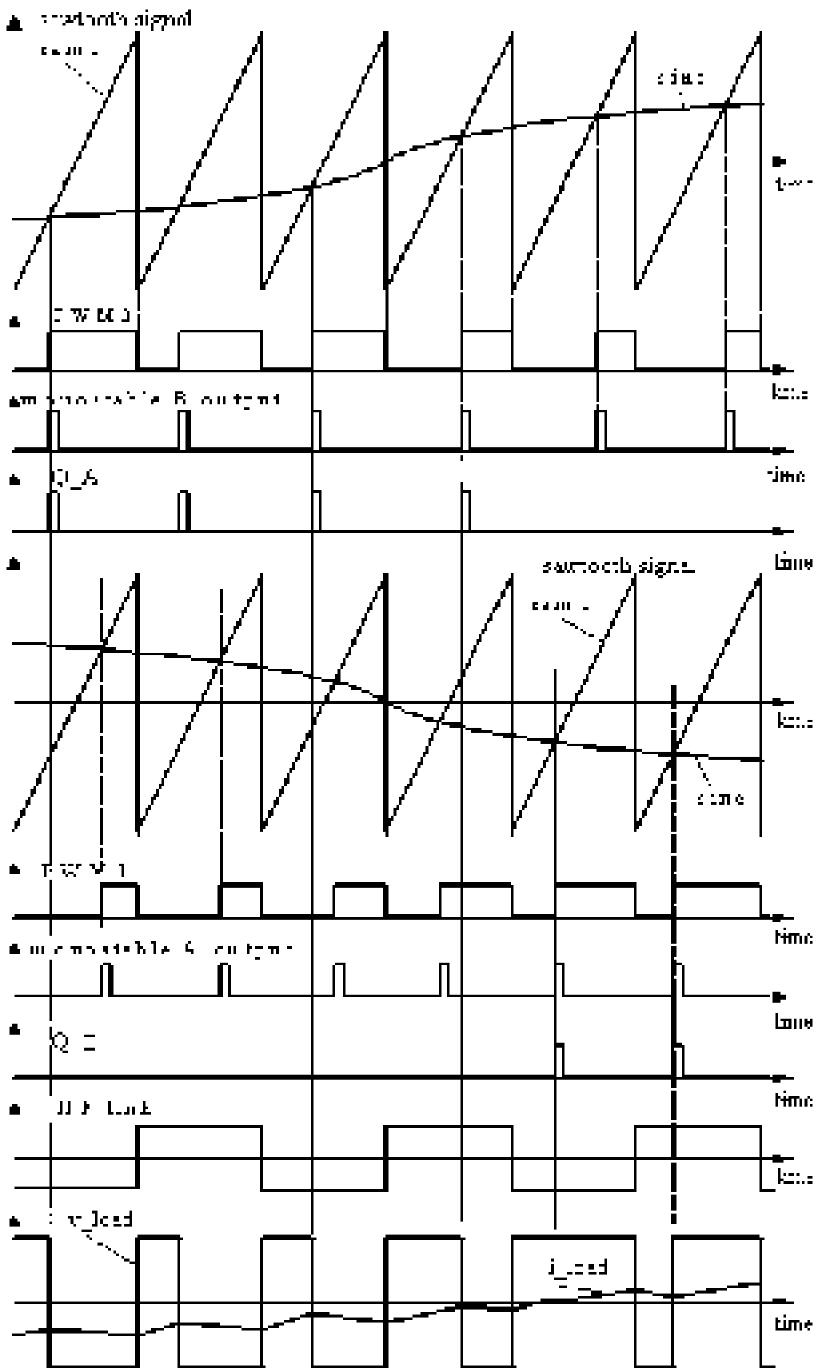

Figure 8. The wave-forms of two carriers PWM sequence generation process

4. Simulation Results

The SPICE® model has been implemented taking in account the circuit shown in Figure 7. The simulation results obtained are shown in Figure 9, where:

- Plot a presents the sine and sawtooth signal;
- Plot b - gate pulses with advanced phase;
- Plot c - gate pulses with delay phase;
- Plot d - load current;
- Plot e - load voltage.

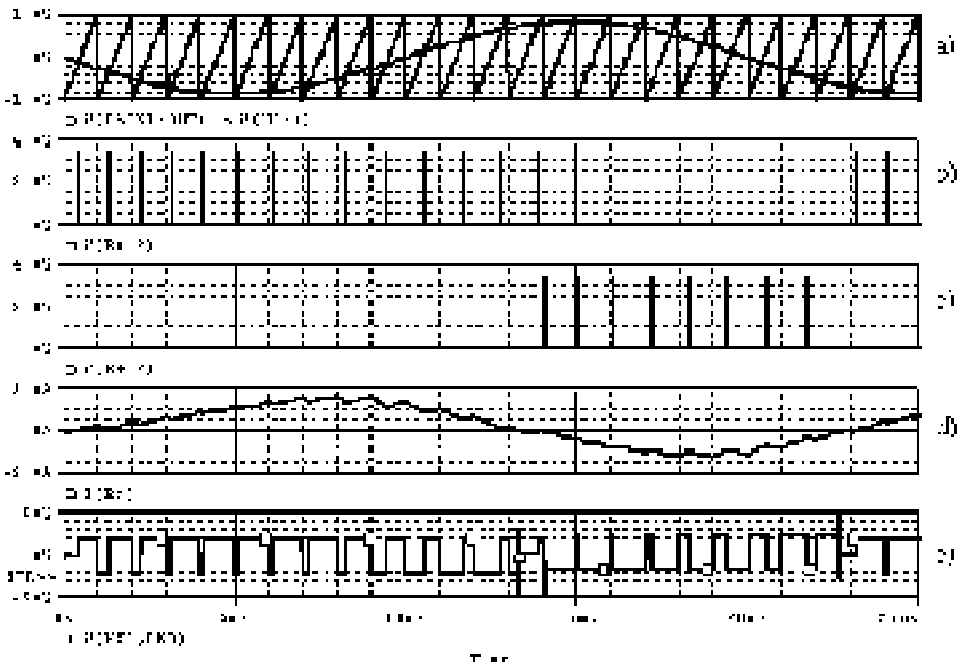

Figure 9. Simulation results using SPICE

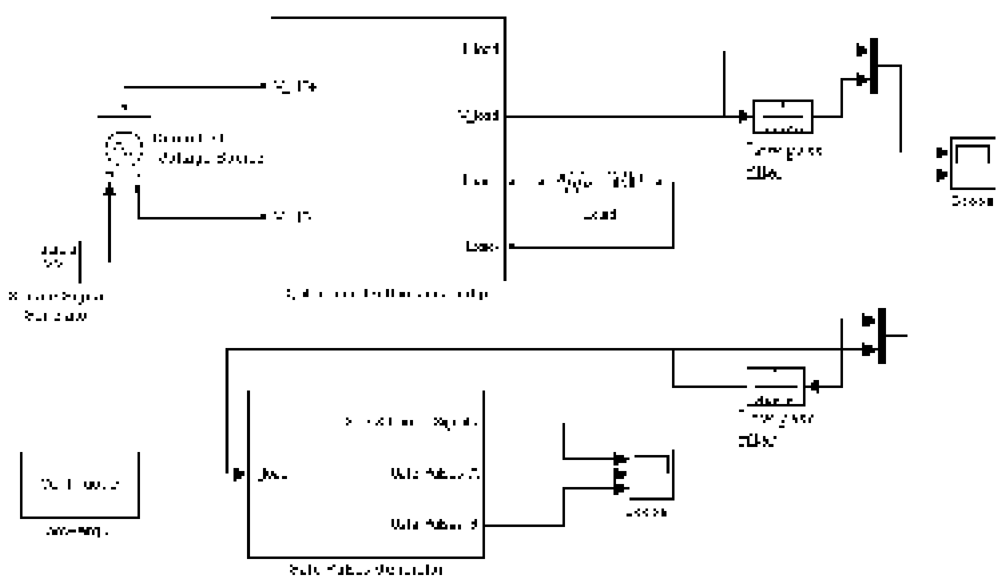

Figure 10. The used Matlab-Simulink® model

It can be seen that output voltage and load current look as it was expected, if it have been taken in account the theoretical assumptions above mentioned.

The Matlab-Simulink® modeling was also used to validate the results obtained with SPICE. The HF AC bus is generated by the Controlled Voltage Source (CVS) using a square signal generator as control signal (Figure 10). The cycloconverter and the two-carrier PWM controller structure are shown in Figure 11 and 12, respectively. The gate pulses generated by the two-carrier PWM controller are shown in Figure 13.

As it was expected, the same simulation results are obtained using Matlab-Simulink® and SPICE®.

In order to further analyze the load dependence of the cycloconverter switching using a two-carrier PWM controller, the thyristor currents are viewed synchronously with the 300 V/ 1 kHz squared CVS (Figure 14), when a synchronized sawtooth carrier (2 kHz) is used in the two-carrier PWM controller.

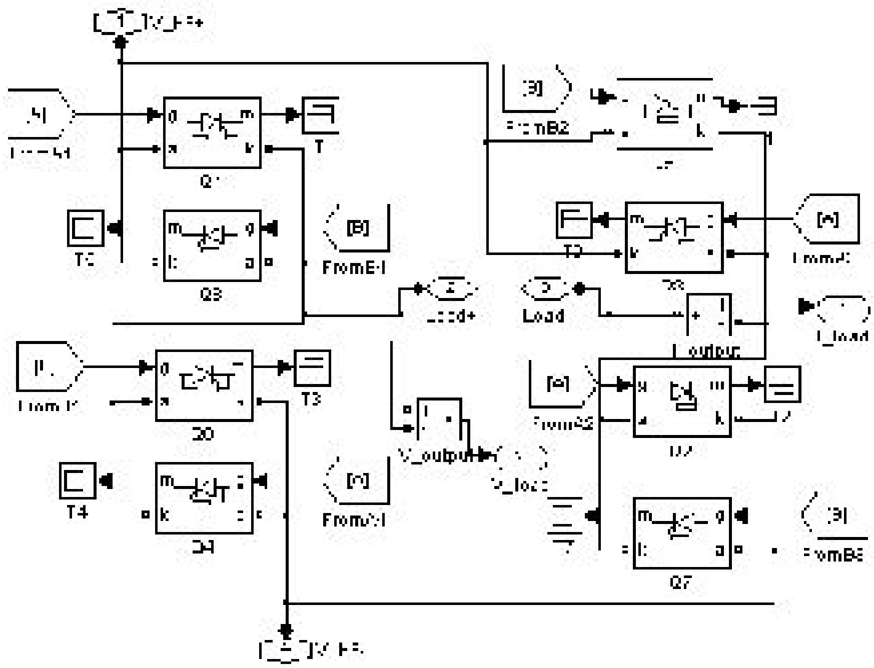

Figure 11. Cycloconverter structure

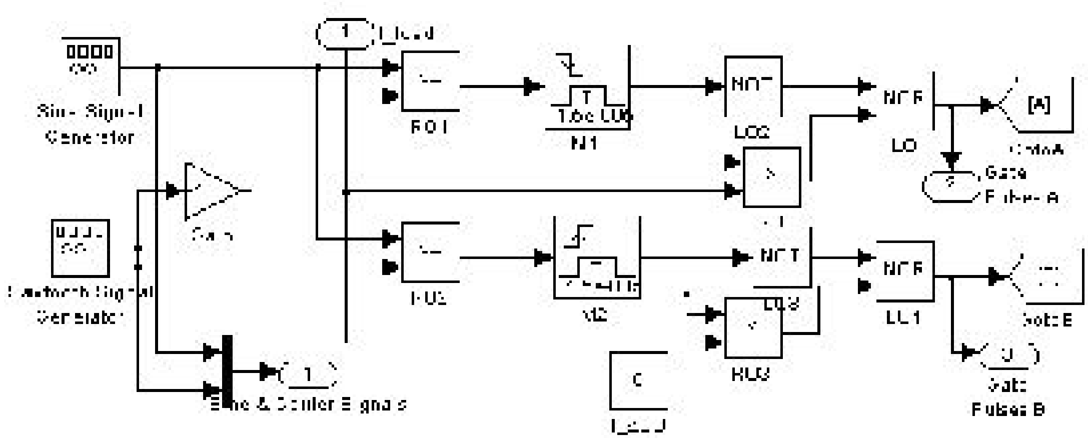

Figure 12. Two-carrier PWM controller structure